Interferometric Astrometry of the Detached White Dwarf-M Dwarf Binary Feige 24 Using HST Fine Guidance Sensor 3: White Dwarf Radius and Component Mass Estimates

G. Fritz Benedict

Barbara E. McArthur

Otto G. Franz

L. H. Wasserman

E. Nelan

See next page for additional authors

Interferometric Astrometry of the Detached White Dwarf-M Dwarf Binary Feige 24 Using HST Fine Guidance Sensor 3: White Dwarf Radius and Component Mass Estimates

Authors

G. Fritz Benedict, Barbara E. McArthur, Otto G. Franz, L. H. Wasserman, E. Nelan, J. Lee, L. W. Fredrick, W. H. Jefferys, W. van Altena, E. L. Robinson, W. J. Spiesman, P. J. Hemenway, R. L. Duncombe, D. Story, A. L. Whipple, and A. Bradley

Terms of Use

INTERFEROMETRIC ASTROMETRY OF THE DETACHED WHITE DWARF—M DWARF BINARY FEIGE 24 USING *HST* FINE GUIDANCE SENSOR 3: WHITE DWARF RADIUS AND COMPONENT MASS ESTIMATES[1]

G. Fritz Benedict,[2] Barbara E. McArthur,[2] Otto G. Franz,[3] L. H. Wasserman,[3] E. Nelan,[4] J. Lee,[7]
L. W. Fredrick,[6] W. H. Jefferys,[7] W. van Altena,[5] E. L. Robinson,[7] W. J. Spiesman,[2] P. J. Shelus,[2]
P. D. Hemenway,[8] R. L. Duncombe,[9] D. Story,[10] A. L. Whipple,[11] and A. Bradley[11]

ABSTRACT

With *Hubble Space Telescope* Fine Guidance Sensor 3 we have determined a parallax for the white dwarf–M dwarf interacting binary, Feige 24. The white dwarf (DA) component has an effective temperature $T_{\mathrm{eff}} \sim 56,000$ K. A weighted average with past parallax determinations ($\pi_{\mathrm{abs}} = 14.6 \pm 0.4$ mas) narrows the range of possible radius values, compared with past estimates. We obtain $R_{\mathrm{DA}} = 0.0185 \pm 0.0008 \, R_\odot$ with uncertainty in the temperature and bolometric correction the dominant contributors to the error. Fine Guidance Sensor 3 photometry provides a light curve entirely consistent with reflection effects. A recently refined model mass-luminosity relation for low-mass stars provides a mass estimate for the M dwarf companion, $M_{\mathrm{dM}} = 0.37 \pm 0.20 \, M_\odot$, where the mass range is due to metallicity and age uncertainties. Radial velocities from Vennes and Thorstensen provide a mass ratio from which we obtain $M_{\mathrm{DA}} = 0.49^{+0.19}_{-0.05} \, M_\odot$. Independently, our radius and recent log g determinations yield 0.44 $M_\odot < M_{\mathrm{DA}} < 0.47 \, M_\odot$. In each case, the minimum DA mass is that derived by Vennes & Thorstensen from their radial velocities and Keplerian circular orbits with $i \leq 90°$. Locating Feige 24 on an (M, R)-plane suggests a carbon core. Our radius and these mass estimates yield a value of γ_{grav} inconsistent with that derived by Vennes & Thorstensen. We speculate on the nature of a third component whose existence would resolve the discrepancy.

Key words: astrometry — binaries: general — stars: distances — stars: individual (Feige 24) — stars: late-type — white dwarfs

1. INTRODUCTION

Feige 24 (=PG 0232+035=HIP 12031) is a white dwarf–red dwarf (M1–M2 V) (Liebert & Margon 1977) binary ($P = 4.23$ days; Vennes & Thorstensen 1994, hereafter VT94) that is described as the prototypical post–common-envelope detached system with a low probability of becoming a cataclysmic variable (CV) within a Hubble time (King et al. 1994; Marks 1994). This object was selected for our *Hubble Space Telescope* (*HST*) parallax program because a directly measured distance could reduce the uncertainty of the radius of one of the hottest white dwarfs. Since the inauguration of this program and the selection of targets over 15 years ago, at least two other groups have measured a parallax for Feige 24 (US Naval Observatory at Flagstaff, Dahn et al. 1988, and *Hipparcos*, Perryman et al. 1997; Vauclair et al. 1997). We outlined the results of a preliminary analysis in Benedict et al. (1999b). Here we discuss our analysis and final results in detail.

Provencal et al. (1998) presented radii derived from *Hipparcos* parallaxes for 21 white dwarfs. In most cases, the dominating error term for the white dwarf radii was the parallax uncertainty. Our parallax of Feige 24, while slow in coming, has provided a fractional parallax uncertainty, $\Delta\pi/\pi$, similar to those in the Provencal et al. (1998) study but for a much hotter, more distant object.

We time-tag our data with a modified Julian Date, MJD = JD − 2,400,000.5. We abbreviate milliarcsecond, mas; white dwarf, DA; and M dwarf, dM, throughout.

2. THE ASTROMETRY

Our astrometric observations were obtained with the Fine Guidance Sensor 3 (FGS 3), a two-axis, white-light interferometer aboard the *HST*. Bradley et al. (1991) provide an overview of the FGS 3 instrument and Benedict et al. (1999a) describe the astrometric capabilities of FGS 3 and typical data acquisition and reduction strategies.

We use the term "pickle" to describe the field of regard of the FGS. The instantaneous field of view of FGS 3 is a $5'' \times 5''$ aperture. Figure 1 shows a finding chart for Feige 24 and our astrometric reference stars in the FGS 3 pickle
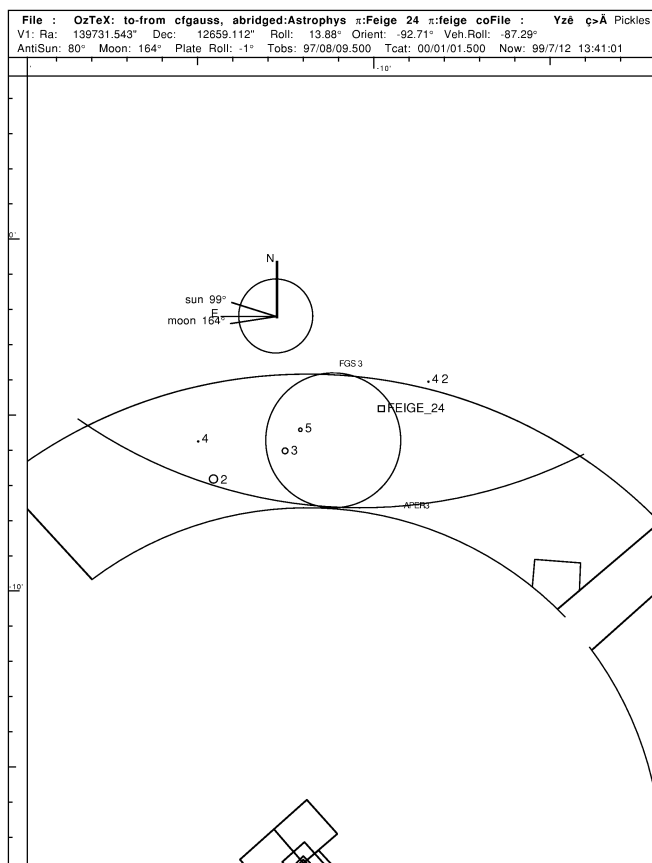
FIG. 1.—Location of reference stars within the FGS 3 field of regard on 1997 August 8. Note the less than ideal placement of the primary science target with respect to the reference frame.

as observed on 1997 August 8. Note the less than ideal placement of the primary science target with respect to the reference frame. The placement of Feige 24 at one side of the distribution of reference stars seems to have produced few adverse astrometric or photometric effects.

2.1. Astrometric Reference Frame

Table 4 provides a list of the observation epochs. Our data reduction and calibration procedures are described in Benedict et al. (1999a) and McArthur et al. (1999). We obtained a total of 71 successful measurements of our reference stars during eight observing runs. For each of these eight observation sets, we determine the scale and rotation relative to the sky, using a GAUSSFIT (Jefferys, Fitzpatrick, & McArthur 1987) model. The orientation of the observation sets is obtained from ground-based astrometry (Monet 1998, hereafter USNO) with uncertainties in the field orientation of $\pm 0°.12$.

Having only eight observation sets and four reference stars precludes us from following our usual practice (Benedict et al. 1999a) of constraining the proper motions and parallaxes to sum to zero ($\sum \mu = 0$ and $\sum \pi = 0$) for the entire reference frame. From a series of solutions, we determined that only reference star 3 has a statistically significant proper motion and parallax. So, we constrain $\mu = 0$ and $\pi = 0$ for reference stars 2, 4, and 5.

We conclude from histograms (Fig. 2) of the reference-star residuals that we have obtained a precision of ~ 1 mas

for each observation. The resulting reference frame "catalog" (Tables 1 and 2) was determined with final errors $\langle \sigma_\xi \rangle = 0.5$ and $\langle \sigma_\eta \rangle = 0.6$ mas.

To determine whether there might be unmodeled but eventually correctable systematic effects at the 1 mas level, we plotted the Feige 24 reference frame X and Y residuals against a number of spacecraft, instrumental, and astronomical parameters. These included (X, Y)-position within the pickle, radial distance from the pickle center, reference-star V magnitude and $B-V$ color, and epoch of observation. We saw no trends other than the expected increase in positional uncertainty with reference-star magnitude.

2.2. Modeling the Parallax and Proper Motion of Feige 24

Spectroscopy of the reference-frame stars was obtained from the WIYN[12] and an estimate of color excess, $E(B-V)$, from Burstein & Heiles 1982. Table 2 shows that the colors of the reference stars and our science target differ, with $\Delta(B-V) \sim -1$. Therefore, we apply the differential correction for lateral color discussed in Benedict et al. (1999a) to the Feige 24 observations and obtain a parallax relative to our reference frame, $\pi_{rel} = 13.8 \pm 0.4$ mas. The proper motion relative to the four astrometric reference stars is listed in Table 3.

Franz et al. (1998) and Benedict et al. (1999a) have demonstrated 1 mas astrometric precision for FGS 3. Table 4 presents our Feige 24 astrometric residuals obtained from the parallax and proper-motion model. Histograms of these residuals are characterized by $\sigma_x = 1.0$ and $\sigma_y = 1.2$ mas. This was slightly larger than expected. To investigate whether or not the larger residuals could be attributed to Feige 24, Figure 3 presents the residuals phased to the VT94 orbital period, $P = 4.23160$ days, with $T_0 = HJD2,448,578.3973$. We find no significant trends in the astrometric residuals. In particular, there is no correlation with the two distinct HST orientations required by the pointing constraints discussed in Benedict et al. (1999a). With any reasonable masses for the DA and dM components, a binary system at this distance with this period could exhibit maximum reflex motion at the 0.5 mas level. This null detection does not place very useful upper limits on the component masses.

Because our parallax for Feige 24 is determined with respect to the reference-frame stars, which have their own parallaxes, we must apply a correction from relative to absolute parallax. The WIYN spectroscopy and the estimated color excess (see Table 2) indicate a reference frame with an average parallax of $\langle \pi_{ref} \rangle = 0.9 \pm 0.4$ mas, where the error is based on the dispersion of the individual spectrophotometric parallaxes. To check our correction to absolute, we compare it with those used in the Yale Parallax Catalog (van Altena, Lee, & Hoffleit 1995, hereafter YPC95; § 3.2). From YPC95, Figure 2, the Feige 24 Galactic latitude, $b = -50°.3$, and the average magnitude for the reference frame, $\langle V_{ref} \rangle = 13.4$, we obtain a correction to absolute of 1.9 mas. Rather than use a galactic model-dependent correction, we adopt the spectroscopically derived value $\langle \pi_{ref} \rangle = 0.9 \pm 0.4$ mas. Applying this correc-
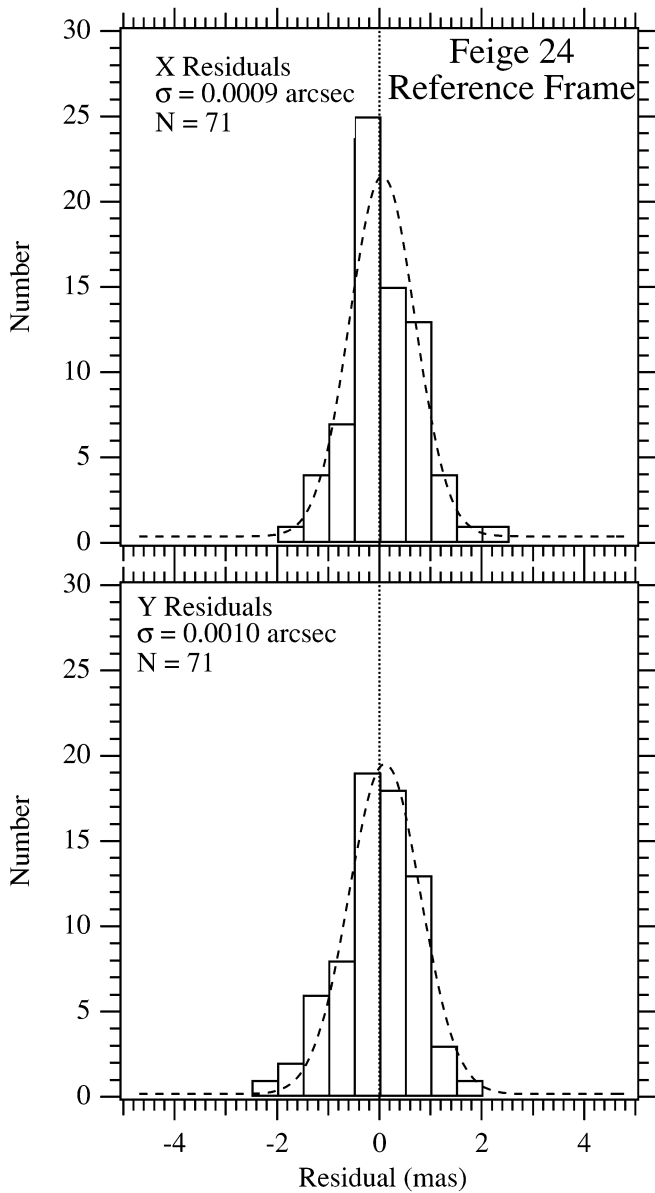

FIG. 2.—Histograms of X and Y residuals obtained from modeling the Feige 24 reference frame to obtain scale, orientation, and offset parameters. Distributions are fit with Gaussians.

FIG. 3.—Astrometric residuals in right ascension (X) and declination (Y) phased to the VT94 orbit (P = 4.23160 days and T_0 = JD 2,448,578.3973). Boxes and open circles denote the two HST orientations, which seem to have no effect on the astrometric residuals. Dashed lines are best-fit sine waves constrained to the VT94 period.

tion results in an absolute parallax of π_{abs} = +14.7 ± 0.6 mas, where the error has equal contributions from the HST FGS observations and the correction to absolute parallax. Finally, we note that our proper motion is smaller than
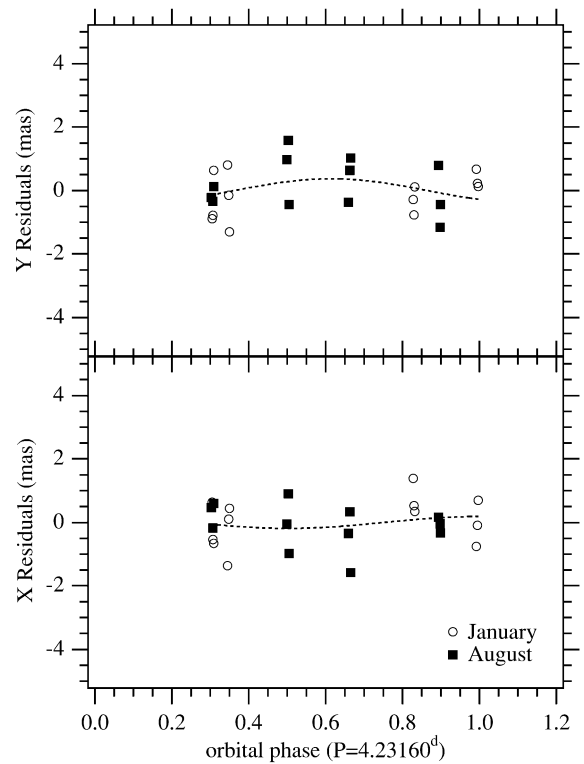
either the Hipparcos or USNO values, for the Hipparcos value is an absolute proper motion, while the USNO and the HST values are relative to their respective reference-frame proper motions. If our reference stars are a representative statistical sample of the parent population, then based on the data in Table III in van Altena (1974), we expect a statistical uncertainty in the mean value of the correction to absolute proper motion (not applied here) of ±6 mas yr^{-1}.

We compare our absolute parallax with previous work in Table 3 and in Figure 4. We adopt for the remainder of this paper the weighted average absolute parallax, $\langle \pi_{abs} \rangle$ = 14.6 ± 0.4 mas, shown as a horizontal dashed line in Figure 4. Weights used are $1/\sigma^2$.

Lutz & Kelker (1973) show that for a uniform distribution of stars, the measured trigonometric parallaxes are strongly biased toward the observer (i.e., too large), render-

TABLE 1

FEIGE 24 REFERENCE FRAME: ASTROMETRY

Reference Star	V	ξ (arcsec)	η (arcsec)	μ_X (arcsec yr^{-1})	μ_Y (arcsec yr^{-1})	π (arcsec)
2[a]	11.59	0.0 ± 0.0004	0.0 ± 0.0004	0	0	0
3	13.38	−118.9943 ± 0.0004	50.4968 ± 0.0004	0.0157 ± 0.0004	0.0014 ± 0.00050	−0.0006 ± 0.0003
4	14.82	27.3168 ± 0.0010	63.5709 ± 0.0010	0	0	0
5	13.66	−144.4703 ± 0.0004	86.9851 ± 0.0005	0	0	0

[a] R.A. 288.087967, decl. 2.898281; J2000.0.

TABLE 2

FEIGE 24 AND ITS REFERENCE FRAME: STELLAR PARAMETERS

Object	V[a]	$B-V$[b]	Spectral Type	M_V	$E(B-V)$[c]	A_V	$m-M$	D (pc)	π_{abs}(mas)
Reference 2......	11.59	1.00	G9 III	0.75	0.03	0.093	10.84	960	0.6
Reference 3......	13.38	0.69	G3 V	4.8	0.03	0.093	8.58	410	1.9
Reference 4......	14.82	0.61	G0 V	4.4	0.03	0.093	10.42	935	0.8
Reference 5......	13.66	0.63	F9 III	1.2	0.03	0.093	12.46	2540	0.3
Feige 24	12.41[d]	−0.20[d]	...	...	...	...	...	...	...

[a] From FGS PMT measures calibrated as per Nelan et al. 1999.
[b] From $B-V = $ f(Sp.T.) $+ E(B-V)$.
[c] From Burstein & Heiles 1982.
[d] From Landolt 1983.

TABLE 3

FEIGE 24 PARALLAX, PROPER MOTION, AND RADIAL VELOCITY

Parameter	Value
HST study duration	2.4 yr
Number of observation sets	8
Number of reference stars	4
Reference stars $\langle V \rangle$	13.4
Reference stars $\langle B - V \rangle$	0.7
HST relative parallax	13.8 ± 0.4 mas
Correction to absolute	0.9 ± 0.7 mas
HST absolute parallax	14.7 ± 0.6 mas
Hipparcos absolute parallax	13.4 ± 3.6 mas
USNO absolute parallax	13.5 ± 2.9 mas
HST proper motion (μ)	71.1 ± 0.6 mas yr^{-1}
Position angle	83°6
Hipparcos μ	85.8 ± 5 mas yr^{-1}
Position angle	84°2
USNO μ	78.4 ± 1.9 mas yr^{-1}
Position angle	88°4
Weighted average absolute parallax	14.6 ± 0.4 mas
$m - M$ (LK bias–corrected)	4.17 ± 0.11
System radial velocity, γ[a]	+62.0 ± 1.4 km s^{-1}
Galactocentric z velocity, W[b]	−37 ± 1.5 km s^{-1}

[a] From VT94.
[b] From γ and HST or Hipparcos μ.

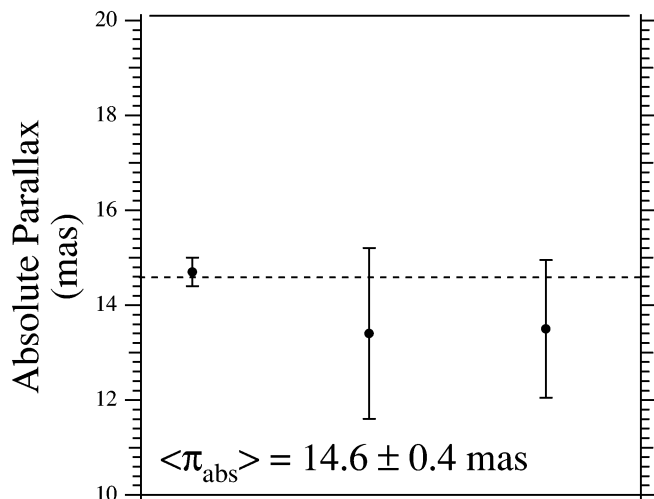
FIG. 4.—Absolute parallax determinations for Feige 24. Left to right: We compare HST, Hipparcos, and USNO (Dahn et al. 1988). Error bars are 1 σ. The dashed line gives the weighted average absolute parallax, $\langle \pi_{abs} \rangle$.

$\langle \pi_{abs} \rangle = 14.6 \pm 0.4$ mas

ing inferred distances and luminosities too small. This bias is proportional to $(\sigma_\pi/\pi)^2$. Using a space density determined for the CV RW Tri (McArthur et al. 1999) and presuming that Feige 24 is a member of that same class of object (binaries containing white dwarfs), we determine an LK-correction of -0.01 ± 0.01 mag. Correcting our distance modulus, we obtain $m - M = 4.17 \pm 0.11$.

2.3. Kinematic Age of the Feige 24 System

From the VT94 systemic radial velocity and either our proper motions or those from Hipparcos (Table 3) we derive the space velocity of Feige 24, 67 ± 1 km s^{-1}. The velocity component perpendicular to the galactic plane, W, is -37 km s^{-1}. Our new parallax places the star 53 pc below the Sun or 61 pc below the galactic plane. An object this far below the galactic plane and continuing to move farther away from the plane so swiftly is more characteristic of a thick disk than a thin disk object (c.f. Thejll et al. 1997).

TABLE 4

HST OBSERVATIONS OF FEIGE 24 AND ASTROMETRIC RESIDUALS

Observation Set	MJD	X Residual	Y Residual
1	49,930.92188	0.0002	0.0008
1	49,930.93750	0.0000	−0.0012
1	49,930.94531	−0.0003	−0.0004
2	49,936.88672	0.0005	−0.0002
2	49,936.90234	−0.0002	−0.0003
2	49,936.91016	0.0006	0.0001
3	50,102.09375	−0.0014	0.0008
3	50,102.10938	0.0001	−0.0002
3	50,102.11719	0.0004	−0.0013
4	50,109.06641	−0.0008	0.0007
4	50,109.07813	−0.0001	0.0002
4	50,109.08594	0.0007	0.0001
5	50,669.78125	−0.0001	0.0010
5	50,669.79688	0.0009	0.0016
5	50,669.80469	−0.0010	−0.0004
6	50,678.92188	−0.0003	−0.0004
6	50,678.93750	0.0003	0.0006
6	50,678.94531	−0.0016	0.0010
7	50,819.28125	0.0014	−0.0003
7	50,819.28906	0.0005	−0.0008
7	50,819.29688	0.0003	0.0001
8	50,821.29688	0.0006	−0.0009
8	50,821.30469	−0.0005	−0.0008
8	50,821.31250	−0.0007	0.0006

Feige 24, if truly a Population I object, has a space velocity 3.5 times the young-disk velocity dispersion. These data suggest that Feige 24 formed earlier than the galactic disk, although subsequent evolution of the DA component is likely quite recent. This may be an instance of past mass transfer in an intermediate Population II object.

3. ASTROPHYSICS OF THE FEIGE 24 SYSTEM

We discuss the consequences of a more precisely determined parallax, calculating some astrophysically relevant parameters for the DA and dM components. These are collected in Table 5. Our goals are the radius and mass of the DA component. We first calculate a radius, then estimate the time since the DA formation event. Component masses have been estimated by VT94. We will revisit this issue later. That we do not substantially improve the mass uncertainty motivates a future direct measurement of the component separation. This one measurement would yield precise masses. A series of measurements would provide individual orbits, possibly illuminating past and future component interactions.

3.1. Estimating the DA Radius

To estimate the DA radius, we require an intrinsic luminosity. From Landolt 1983, we obtain a system total magnitude, $V_{tot} = 12.41 \pm 0.01$. The magnitude of the white dwarf is critical and difficult to obtain, because the M dwarf always contributes flux. Holberg, Basile, & Wesemael (1986) derive $V_{DA} = 12.56 \pm 0.05$ using IUE spectra. They ratio Feige 24 with other hot DA, G191 B2B, GD246, and HZ43. From the DA magnitude and total magnitude, we obtain $V_{dM} = 14.63 \pm 0.05$ and $\Delta V = 2.07$. We assume $A_V = 0$ for Feige 24 at $d = 69$ pc, consistent with our adopted $A_V = 0.09$ for the reference frame at an average distance $d = 1600$ pc (Table 2). The LK bias–corrected distance modulus $(m - M = 4.17 \pm 0.11)$ then yields absolute magnitudes $M_V = 10.46 \pm 0.12$ for the red dwarf companion and $M_V = 8.39 \pm 0.12$ for the DA.

A recently determined temperature of the Feige 24 DA, taking into account non-LTE and heavy element effects (Barstow, Hubeny, & Holberg 1998), is $T_{eff}^{DA} = 56,370 \pm 1000$ K. This temperature yields a radius via differential comparison with the Sun. This procedure requires a bolometric magnitude and hence a bolometric correction. We could adopt the bolometric correction BC = −4.88, generated by Bergeron, Wesemael, & Beauchamp (1995) from a pure hydrogen DA model with log $g = 8$ convolved with a V bandpass, but for Feige 24 log $g = 8$ does not hold; neither is Feige 24 pure hydrogen.

Flower (1996) provides bolometric corrections for normal stars up to $T_{eff} \sim 54,000$ K. From Flower (1996, Fig. 4) the relationship between log T_{eff} and the BC is linear for $T_{eff} > 25,000$ K. Hotter stars lie on the Rayleigh-Jeans tail of the blackbody curve, where flux is roughly proportional to T_{eff}, not T_{eff}^4. A small linear extrapolation yields BC = −4.82 ± 0.06 for the Feige 24 DA. The BC error comes from the uncertainty in T_{eff}^{DA}.

Because a DA with some heavy elements in its atmosphere radiates more like a hot normal star than a pure hydrogen DA, we choose the Flower correction rather than the model correction. We are also encouraged by the near equality of the BC values from observation and theory.

We obtain a DA bolometric luminosity $M_{bol}^{DA} = M_V$ + BC = 3.57 ± 0.13. R_{DA} follows from the expression

$$M_{bol}^{\odot} - M_{bol}^{DA} = 10 \log(T_{eff}^{DA}/T_{eff}^{\odot}) + 5 \log(R_{DA}/R_{\odot}), \quad (1)$$

where we assume for the Sun $M_{bol}^{\odot} = +4.75$ and $T_{eff}^{\odot} = 5800$ K. We find $R_{DA} = 0.0180 \pm 0.0013\ R_{\odot}$, following the error analysis of Provencal et al. 1998. The primary sources of error for this radius are the bolometric correction and the T_{eff}^{DA}.

A second approach to deriving R_{DA} involves the V-band average flux, H_V, discussed in Bergeron et al. (1995). They list H_V^{DA} as a function of temperature for, again, the pure hydrogen model with log $g = 8$. If we can determine a value for $H_V^{\odot}$, we can derive R_{DA} from

$$R_{DA} = (H_V^{\odot}/H_V^{DA})10^{-0.4(M_V^{DA} - M_V^{\odot})}, \quad (2)$$

where $M_V^{DA} = 8.39 \pm 0.12$ comes from our parallax and $M_V^{\odot} = 4.82$ is assumed. We obtain $H_V^{\odot}$ by convolving the Bessell (1990) V-band response with the solar spectral

TABLE 5
FEIGE 24 ASTROPHYSICAL QUANTITIES

Parameter	Value	Source
V_{tot}	12.41 ± 0.01	Landolt 1983
$B-V$	−0.20 ± 0.01	Landolt 1983
V_{DA}	12.56 ± 0.05	Holberg et al. 1986
V_{dM}	14.63 ± 0.05	V_{tot} and V_{DA}
A_V	0	Reference frame $\langle B-V \rangle$, spectral type (Table 2)
$m - M$ (LK bias–corrected)	4.17 ± 0.11	This paper
dM M_V	10.46 ± 0.12	$m - M$
dM spectral type	M2 V	dM M_V, Henry et al. 1994
M_{dM}	0.29−0.43 $M_{\odot}$	dM M_V, Baraffe et al. 1998, $M_{DA,Kep}$
DA M_V	8.39 ± 0.12	$m - M$
DA BC	−4.82 ± 0.06	Flower 1996
M_{bol}^{DA}	3.57 ± 0.13	= DA M_V + BC
T_{eff}^{DA}	56,370 ± 1000K	Barstow et al. 1998
R_{DA}	0.0185 ± 0.0008 $R_{\odot}$	This paper
M_{dM}/M_{DA}	0.63 ± 0.04	K_{DA}/K_{dM}, VT94
M_{DA}	$0.49^{+0.19}_{-0.05}\ M_{\odot}$	M_{dM}, K_{DA}/K_{dM}, $M_{DA,Kep}$
M_{DA}	0.44−0.47 $M_{\odot}$	log g, $M_{DA,Kep}$

distribution listed in Allen (1973). We calculate $H_V^\odot = 6.771 \times 10^5$ ergs cm^{-2} s^{-1} Å^{-1} str^{-1}. We obtain for $T_{eff} = 56{,}370$ K an $R_{DA} = 0.0188 \pm 0.0010$.

A weighted average of the two independent determinations provides $R_{DA} = 0.0185 \pm 0.0008 \, R_\odot$, where the error is certainly underestimated because of unknown systematic effects. Parallax is no longer a significant source of error for the radius determination. Comparing with the results presented in Provencal et al. (1998, Fig. 7), we find Feige 24 to have a radius larger than any other white dwarf.

With a temperature $T_{eff} \sim 56{,}000$ K, the time since the DA formation event is unlikely to be longer than 1.5 Myr. This conclusion is drawn from the DA cooling tracks as a function of mass calculated by M. Wood, detailed in Sion (1999, Fig. 7). These models also indicate that the DA mass must satisfy $M_{DA} \geq 0.4 \, M_\odot$ to remain near this lofty T_{eff} for longer than 3×10^5 yr.

3.2. Estimating the White Dwarf Mass

Before estimating M_{DA}, we review the VT94 minimum component masses from their radial velocities and the Kepler relation for total system mass, separation, and period. Then we estimate the DA mass using two different approaches. We first attempt to determine the most likely dM mass. The VT94 radial velocity amplitude ratio then provides the DA mass. The second, independent mass estimate follows from our derived radius, along with the DA atmospheric parameter, log g, obtained through spectroscopy. Our DA mass estimate will differ little from VT94 and, if better, is so only by virtue of more recent dM models and DA atmospheric parameters.

3.2.1. Minimum Component Masses from Binary Radial Velocities

The system total lower mass limit can be set by the VT94 radial velocities and the Kepler relation for mass, separation, and period. VT 94 gives us the velocities along each component orbit, the fact that each orbit is circular (from the pure sine wave fits to the velocity curves), and the period, the time it takes to travel around each orbit. Assuming an edge-on system ($i = 90°$), one that can produce the full vector amount of radial velocity amplitude measured by VT94, the minimum system mass is $M_{tot} = 0.73 \, M_\odot$. From the VT94 mass ratio, $M_{dM}/M_{DA} = 0.63 \pm 0.04$, we obtain the DA mass limit, $M_{DA,Kep} \geq 0.44 \, M_\odot$, and the dM mass limit, $M_{dM,Kep} \geq 0.26 \, M_\odot$. No smaller masses can produce the observed radial velocities for orbits of these known sizes. At $d = 68.5$ pc, an edge-on system with minimum mass would separate the components by 672 μas or 9.9 $R_\odot$.

3.2.2. Inclination from the Light Curve

VT 94 find Hα equivalent width variations that phase with the orbital period. These show a maximum at $\phi = 0.5$. Photometric variations of Feige 24 might be detectable, because the photometric capabilities of FGS 3 approach a precision of 0.002 mag (Benedict et al. 1998). Figure 5 shows the flat-fielded counts and the corresponding differential instrumental magnitudes as well as a sine wave fit with amplitude and phase as free parameters. There is a clear photometric signature with a peak-to-peak amplitude of 0.028 mag, showing maximum system brightness at phase $\phi = 0.58 \pm 0.09$. Given the sparse coverage, this phase at maximum is not surprisingly different from the Hα equivalent width maximum seen at $\phi = 0.5$.
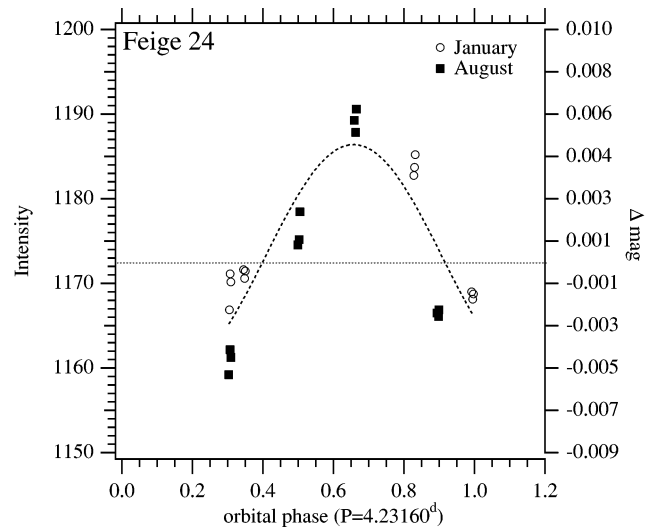

FIG. 5.—Flat-fielded intensity (the filter, F583W, has a bandpass centered on 583 nm, with 234 nm FWHM) and differential instrumental magnitudes phased to the VT94 orbit ($P = 4.23160$ days and $T_0 = $ JD2,448, 578.3973). Squares and circles denote the two *HST* orientations, which seem to have no effect on the photometry. The dashed line is a best-fit sine wave constrained to the VT94 period.

A likely mechanism for producing the single-peaked orbital light curve is heating of the dM star by the white dwarf (the reflection effect). As the dM star orbits the white dwarf, its heated face is alternately more or less visible, increasing and decreasing the observed flux from Feige 24 once per orbit. To test this hypothesis, we calculated model light curves using an updated version of the light-curve synthesis program described by Zhang, Robinson, & Nather (1986). We initially adopted $T_{eff} = 56{,}370$ K and $R = 0.0185 \, R_\odot$ for the white dwarf, $T_{eff} = 3800$ K and $R = 0.52 \, R_\odot$ for the M1–2M V star, and 4.8×10^{-2} AU (10.3 $R_\odot$) for the separation of their centers of mass, and then we adjusted the temperature of the dM star so that it contributed 13.5% of the V flux from the system. The peak-to-peak amplitudes of the resulting model light curves are a function of orbital inclination, topping out at ~ 0.025 mag for $i = 90°$, and can easily be made to agree in amplitude and shape with the observed light curve.

This photometric behavior is entirely consistent with reflection effects. We find that the quality of the observed light curve is, however, inadequate to improve the parameters of the system, particularly the inclination. We have not sufficiently sampled the expected flat section of the light curve (near $\phi = 0$). Nevertheless, these results do provide quantitative evidence that (1) the orbital light curve is caused by heating and (2) the heating is consistent with the radius and temperature we have derived for the white dwarf—a useful external check on our results.

3.2.3. DA Mass from the M Dwarf

The dM absolute magnitude ($M_V = 10.46 \pm 0.12$) implies a spectral type M2V (Henry, Kirkpatrick, & Simons 1994), consistent with Liebert & Margon (1977). The absolute magnitude of an M dwarf star depends not only on mass but also on age (evolutionary stage) and chemical composition. Baraffe et al. (1998) have produced a grid of models that vary metallicity, [M/H], and helium abundance, Y. We
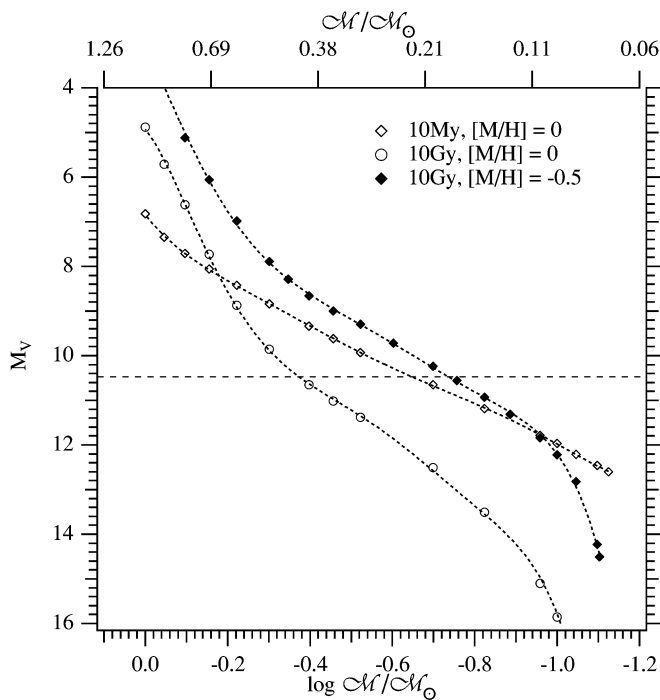
FIG. 6.—M dwarf absolute magnitude as a function of mass from the stellar evolution models of Baraffe et al. (1998). A wide range of masses, ages, and metallicities can result in the derived dM absolute magnitude, $M_V = 10.46$ (horizontal line). Note that at a given mass, a low-metallicity ([M/H] = −0.5) star is always brighter than a high-metallicity ([M/H] = 0.0) star, for $M > 0.1\ M$.
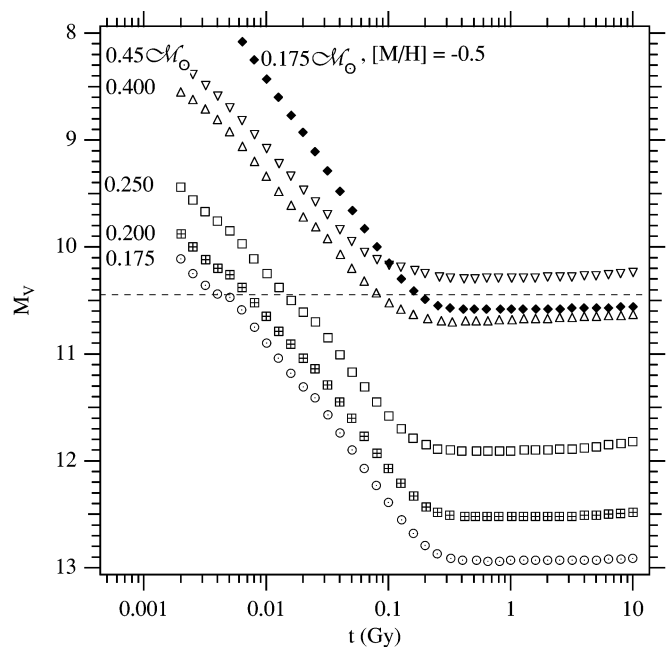

FIG. 7.—Time variation of absolute magnitude for M dwarfs of various masses taken from the stellar evolution models of Baraffe et al. (1998). Empty symbols represent solar metallicity; filled represent low metallicity ([M/H] = −0.5). Note that the higher mass stars remain near the computed M dwarf absolute magnitude, $M_V = 10.46$ (dashed line), far longer than the lower mass stars. A low-metallicity star with $M_{dM} = 0.175\ M_\odot$ is brighter than a solar metallicity star with $M_{dM} = 0.40\ M_\odot$.

plot in Figure 6 their mass-luminosity curves for dwarfs of ages 10 Myr and 10 Gyr with [M/H] = 0 and of age 10 Gyr with [M/H] = −0.5, all with solar helium abundance. The complete grid of Baraffe et al. models shows that M dwarfs in the mass range $0.175\ M_\odot \leq M_{dM} \leq 0.43\ M_\odot$ with $-0.5 < [M/H] < 0$ have $M_V = 10.46$ at some time in their evolution from 10 Myr to 10 Gyr.

The dM mass now depends on metallicity and how quickly an M dwarf of a given mass decreases in brightness. Figure 7 shows the dependence of brightness on mass, age, and metallicity. These Baraffe et al. models indicate that solar metallicity stars with higher mass remain near $M_V = 10.46$ far longer than low-mass stars. However, kinematically, Feige 24 is more likely to be old and of lower than solar metallicity than young and of normal metallicity. First adopting the 10 Gyr model, [M/H] = 0, and calculated absolute magnitude, we estimate the dM star mass $M_{dM} = 0.43 \pm 0.08\ M_\odot$, because that mass remains at $M_V = 10.46$ for a larger fraction of the total lifetime than any other. However, if we accept the kinematic suggestion of allegiance to a thick-disk population, then [M/H] < 0 is more likely. Assuming [M/H] = −0.5 results in a dM star mass $M_{dM} = 0.185 \pm 0.08\ M_\odot$.

Radial velocities from VT94 (dM from Kitt Peak, DA from *IUE*) provide the velocity amplitude ratio, $K_{DA}/K_{dM} = 0.63 \pm 0.04 = M_{dM}/M_{DA}$. From the total possible dM mass range, $0.185\ M_\odot < M_{dM} < 0.43\ M_\odot$, and the mass ratio, we derive a DA mass range, $0.29\ M_\odot < M_{DA} < 0.68\ M_\odot$. Applying the limit, $M_{DA,Kep} \geq 0.44\ M_\odot$, we obtain $0.44\ M_\odot < M_{DA} < 0.68\ M_\odot$. Keplerian lower limits argue for a dM star mass $0.26\ M_\odot < M_{dM} < 0.43\ M_\odot$, a range consistent with a metallicity slightly less than solar and an age in excess of 0.3 Gyr (Fig. 7).

3.2.4. DA Mass from Atmospheric Parameters

The dM star does not provide a particularly precise DA mass estimate. If one knows the surface gravity, g, and the radius, R, the mass can be obtained through

$$M = gR^2/G,\qquad(3)$$

where G is the gravitational constant. The quantity $\log g$ comes from analysis of the line profiles in spectra. Recent determinations include the following: Marsh et al. (1997), $\log g = 7.53 \pm 0.09$; Kidder (1991), $\log g = 7.45 \pm 0.51$; Vennes et al. (1997), $\log g = 7.2 \pm 0.07$; Finley, Koester, & Basri (1997), $\log g = 7.17 \pm 0.15$; and Barstow et al. 1998, $\log g = 7.36 \pm 0.12$. The full range of the measures and equation (3) yield the range of mass values $0.21\ M_\odot \leq M_{DA} \leq 0.47\ M_\odot$. Applying the limit $M_{DA,Kep} \geq 0.44\ M_\odot$ eliminates nearly all of these mass determinations. In this case, our radius and the Kepler limit indicate that $\log g$ should be at the high end of these measures.

3.3. White Dwarf Composition

We next place Feige 24 on a white dwarf mass-radius diagram (Fig. 8). We plot our two independently determined mass ranges against our adopted radius, $R_{DA} = 0.0185 \pm 0.0008\ R_\odot$. We represent the radius error by the two horizontal short-dash–long-dashed lines. The top thick horizontal bar shows the M_{DA} determined from atmospheric parameters. Only the largest $\log g$ at the largest radius produces masses in excess of the Keplerian limit. The thick bar at $R_{DA} = 0.0185\ R_\odot$ indicates the M_{DA} range derived through the dM mass estimates. For this determination, the mass error bars indicate the range of ages and [M/H] discussed in § 3.2.3. For any dM older than 1–2 Gyr, the lower masses are associated with lower metallicity. The vertical dotted line shows the lowest possible M_{DA} that can
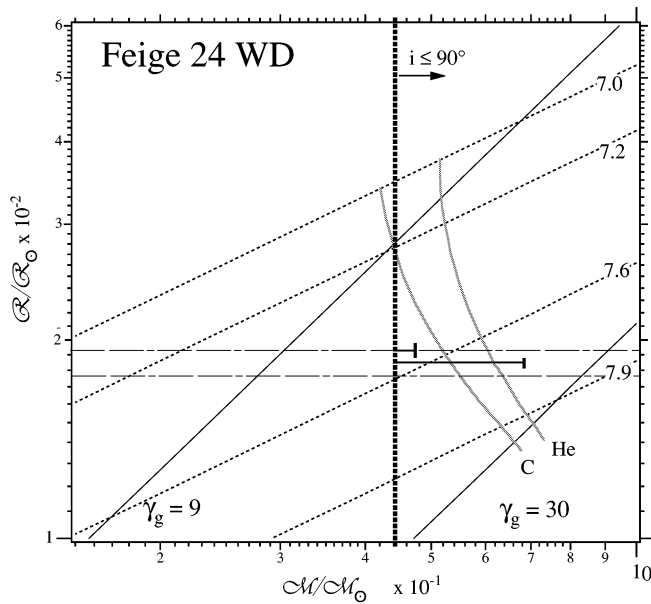
FIG. 8.—Feige 24 mass and radius on a DA mass-radius map, showing the lowest possible M_{DA} from Keplerian considerations (*vertical dotted line*). The radius error is represented by the two horizontal short-dash–long-dashed lines. The upper horizontal bar shows the M_{DA} determined from atmospheric parameters. Only at the largest radius (lowest temperature) and largest $\log g$ do we obtain a DA mass in excess of the Keplerian limit. The lower horizontal bar, at $R_{DA} = 0.0185\ R_\odot$, indicates the M_{DA} range derived through the dM. We also plot several values of $\log g$ (*dashed lines*) and γ_{grav} (*solid lines*). The curves represent carbon and helium and DA models from Vennes et al. (1995). A carbon-core DA is somewhat more likely than a helium-core DA.

produce the observed VT94 radial velocity amplitudes for an edge-on orientation of this binary system. We also plot several values of $\log g$ (*dashed*) and γ_{grav} (*solid*). The curves in Figure 8 are for carbon and helium DA models from Vennes, Fontaine, & Brassard (1995). While uncertain, a carbon-core DA seems more likely than a pure helium-core DA.

4. DISCUSSION

While our estimated dM and DA masses differ little from those given by VT94, our DA radius differs substantially. VT94 note the difference between their minimum radius, $R_{DA} = 0.028\ R_\odot$, and that predicted by the Dahn et al. (1988) parallax. This discrepancy is exacerbated by the two new parallax determinations (*HST* and *Hipparcos*) folded into our weighted average parallax.

VT94 derive a DA gravitational redshift, $\gamma_{grav} = 8.7 \pm 2$ km s^{-1}, from the measured mean velocities for the dM and DA. Combined with our $R_{DA} = 0.0185\ R_\odot$, this γ_{grav} suggests a forbidden DA mass, $M_{DA} \sim 0.3\ M_\odot$. Reducing the mass of the DA component could reconcile the VT94 $\log g$ and γ_{grav} with our radius.

We speculate that a third component in the Feige 24 system, a low-mass companion to the DA star, could preserve the total system mass and lower the DA mass. If all components are coplanar, the VT94 DA radial velocities apply strict limits to this reconciliation, because too high a mass for component C would show up as large residuals. We estimate from the scatter that a radial velocity amplitude of ± 10 km s^{-1} could "hide" in the VT94 DA radial velocity measurements. Stellar dynamics applies yet another constraint. Holman & Wiegert (1999) parameterize

the stability of tertiary companions as a function of stellar component A and B mass function, $\mu = M_A/(M_A + M_B)$, and AB binary orbit ellipticity, e. With $e = 0$ and $\mu = 0.39$, we find (from their Table 3) that component C must have an orbital semimajor axis less than 0.3 times that of AB.

Insisting that $M_{DA} = 0.30\ M_\odot$ (this mass—with our radius—would produce the upper limit VT94 $\gamma_{grav} = 10.7$ km s^{-1}) requires $M_C = 0.14\ M_\odot$ ($M_A + M_C = 0.44\ M_\odot$). To hide the C component from the radial velocity technique requires a very low AC inclination, nearly face-on. However, noncoplanarity reduces the size of the stable AC semimajor axis even further (Weigert & Holman 1997; Pendleton & Black 1983). As an example, suppose component C must have an orbital semimajor axis of 0.1 or less than that of AB to ensure stability. An AC period, $P = 0.18$ days (4.3 hr), and $i = 6°$ would produce a radial velocity signature of about ± 10 km s^{-1}. Finally, the mass-luminosity relation of Henry et al. (1999) would predict $M_V^C = 14.0$, hence, $V_C \sim 17.2$, likely undetectable in any of the spectra analyzed for radial velocities. Have we postulated a new CV, one that should show evidence of mass transfer and all the associated phenomena? A recent review of CVs (Beuermann 2000) indicates that the putative component C ($M_C = 0.14\ M_\odot$) would have to orbit much closer ($P \sim 1.5$ hr) to the DA primary before filling its Roche lobe and producing the characteristic signature of a CV.

Finally, we note that our radius differs little from that derived by VT94 from the only trigonometric parallax then available (Dahn et al. 1988). The unresolved inconsistency between radii (derived from direct parallaxes) and surface gravities (derived from minimum mass and those radii) illuminates the need for high-angular resolution observations and direct mass determinations.

The Feige 24 DA mass will rest on an age- and metallicity-dependent lower main-sequence mass-luminosity relationship or still uncertain $\log g$ measurements until the component separations are measured directly. Resolving the inconsistencies between the DA mass estimates (involving dM stellar models and uncertain temperatures, $\log g$, and bolometric corrections) requires astrometry, both to reduce the parallax uncertainty further and, more importantly, to resolve spatially this system. Astrometrically derived orbital parameters will provide unambiguous and precise mass determinations for both components. They may also offer insight regarding past and future component interactions.

This system and dozens more like it are ideal targets for the *Space Interferometry Mission* (*SIM*).[13] Feige 24, at a distance of 69 pc with $P = 4.23$ days, has a total component separation on the order of 700 μas. The component orbits are much larger than the expected *SIM* measurement limits. Because shortward of 700 nm, 70%–80% of the system flux is contributed by the DA (Thorstensen et al. 1978), the wide *SIM* bandpass and spectral resolution should allow measurement of positions, magnitudes, and colors for both components, even with $\Delta V \sim 2$.

Once launched, *SIM* will provide crucial astrometry for this and similar systems at 10 times the distance (determined by target magnitude, not astrometric precision). *SIM* measurements of this system along with many other binaries will provide data to create an age- and

---

[13] See http://sim.jpl.nasa.gov.

metallicity-dependent mass-luminosity relationship of exquisite accuracy.

5. CONCLUSIONS

1. The weighted average of three independent parallax measurements yields a distance to the dM + DA binary Feige 24 of $D = 68.4^{+2.0}_{-1.9}$ pc with $\sigma_D/D = 2.8\%$.

2. We estimate the radius of the DA component using two methods. The first requires either a model-dependent bolometric correction or one that derives from hot, normal stars. The second utilizes a model-dependent V-band average flux, H_V. The two results agree within their errors and yield a weighted average $R_{DA} = 0.0185 \pm 0.0008\ R_\odot$, where the most significant contributions to the error are the uncertain T_{eff}^{DA} and the BC. This radius is larger than that of any of the DAs discussed in Provencal et al. (1998).

3. FGS photometry provides quantitative evidence that the orbital light curve is caused by heating of the dM component by the DA. That signature is consistent with the assumed temperature and the radius we have derived for the white dwarf.

4. The radial velocity amplitudes measured by VT94, amplitude ratios, and the assumption of Keplerian circular motion exclude $M_{DA,Kep} < 0.44\ M_\odot$ and $M_{dM,Kep} < 0.26\ M_\odot$.

5. We estimate the dM component mass, $0.26\ M_\odot < M_{dM} < 0.43\ M_\odot$, from the Baraffe et al. (1998) stellar evolution models, a lower limit from Keplerian circular orbits, and the VT 94 radial velocities. The upper range is due to unknown age and metallicity, [M/H]. A DA mass range ($0.44\ M_\odot < M_{DA} < 0.68\ M_\odot$) follows directly from the VT94 radial velocity amplitudes.

6. We determine M_{DA} from our R_{DA} and a rather wide range of spectroscopically determined $\log g$ values. This approach yields $0.44\ M_\odot \le M_{DA} \le 0.47\ M_\odot$, where again the lower limit is imposed by $M_{DA,Kepler} > 0.44\ M_\odot$.

7. We plot these DA component mass ranges in the (M, R)-plane. With the assistance of the hard lower mass limit and carbon and helium DA M-R models from Vennes et al. 1995, we identify Feige 24 as a carbon-core DA. A pure helium-core DA seems less likely.

8. Noting that our radius and the minimum possible M_{DA} are inconsistent with the VT94 value of γ_{grav}, we explore the possibility of a tertiary component. Component C, orbiting a common center of mass with the DA, having a period in the range $1.5\ hr < P < 5\ hr$ with the orbit plane nearly face-on, could reduce the DA mass to $M_{DA} = 0.30\ M_\odot$ and not produce any observational evidence.

9. *SIM* will be able to measure the orbits of each known component and provide directly measured dynamic masses for both. Orbit size and precise shape may provide information on the nature of past and future interactions between the two components. *SIM* would also detect a tertiary, if present.

REFERENCES

Allen, C. W. 1983, Astrophysical Quantities, (3d ed.; London: Athlone)
Baraffe, I., Chabrier, G., Allard, F., & Hauschildt, P. H. 1998, A&A, 337, 403
Barstow, M. A., Hubeny, I., & Holberg, J. B. 1998, MNRAS, 299, 520
Benedict, G. F., et al. 1999a, AJ, 118, 1086
———. 1999b, in ASP Conf. Ser. 194, Working on the Fringe: Optical and Interferometry from Ground and Space, ed. S. Unwin & R. Stachnik (San Francisco: ASP), 38
———. 1998, AJ, 116, 429
Bergeron, P., Wesemael, F., & Beauchamp, A. 1995, PASP, 107, 1047
Bessell, M. S. 1990, PASP, 102, 1181
Beuermann, K. 2000, New A. Rev., in press
Bradley, A., Abramowicz-Reed, L., Story, D., Benedict, G., & Jefferys, W. 1991, PASP, 103, 317
Burstein, D., & Heiles, C. 1982, AJ, 87, 1165
Dahn, C. C., et al. 1988, AJ, 95, 237
Finley, D. S., Koester, D., & Basri, G. 1997, ApJ, 488, 375
Flower, P. J. 1996, ApJ, 469, 355
Franz, O. G., et al. 1998, AJ, 116, 1432
Henry, T. J., Franz, O. G., Wasserman, L. H., Benedict, G. F., Shelus, P. J., Ianna, P. A., Kirkpatrick, J. D., & McCarthy, D. W. 1999, ApJ, 512, 864
Henry, T. J., Kirkpatrick, J. D., & Simons, D. A. 1994, AJ, 108, 1437
Holberg, J. B., Basile, J., & Wesemael, F. 1986, ApJ, 306, 629
Holman, M., & Wiegert, P. 1999, AJ, 117, 621
Jefferys, W., Fitzpatrick, J., & McArthur, B. 1987, Celest. Mech., 41, 39
Kidder, K. M. 1991, Ph.D. thesis, Univ. Arizona
King, A. R., Kolb, U., De Kool, M., & Ritter, H. 1994, MNRAS, 269, 907

Landolt, A. U. 1983, AJ, 88, 439
Liebert, J., & Margon, B. 1977, ApJ, 216, 18
Lutz, T. E., & Kelker, D. H. 1973, PASP, 85, 573
Marks, P. B. 1994, in Cataclysmic Variables, ed. A. Bianchini, M. Della Valle, & M. Orio (Dordrecht: Kluwer), 535
Marsh, M. C., et al. 1997, MNRAS, 286, 369
McArthur, B. E., et al. 1999, ApJ, 520, L59
Monet, D. G. 1998, BAAS, 193, No. 112.003 (USNO)
Nelan, E. 1999, Fine Guidance Sensor Instrument Handbook (version 8; Baltimore: STScI)
Pendleton, Y. J., & Black, D. C. 1983, AJ, 88, 1415
Perryman, M. A. C., et al. 1997, A&A, 323, L49
Provencal, J. L., Shipman, H. L., Høg, E., & Thejll, P. 1998, ApJ, 494, 759
Sion, E. M. 1999, PASP, 111, 532
Thejll, P., Flynn, C., Williamson, R., & Saffer, R. 1997, A&A, 317, 689
Thorstensen, J. R., Charles, P. A., Bowyer, S., & Margon, B. 1978, ApJ, 223, 260
van Altena, W. 1974, AJ, 79, 826
van Altena, W. F., Lee, J. T., & Hoffleit, E. D. 1995, Yale Parallax Catalog (4th ed.; New Haven, CT: Yale Univ. Obs.) (YPC95)
Vauclair, G., Schmidt, H., Koester, D., & Allard, N. 1997, A&A, 325, 1055
Vennes, S., Fontaine, G., & Brassard, P. 1995, A&A, 296, 117
Vennes, S., Thejll, P. A., Galvan, R. G., & Dupuis, J. 1997, ApJ, 480, 714
Vennes, S., & Thorstensen, J. R. 1994, AJ, 108, 1881 (VT94)
Wiegert, P. A., & Holman, M. J. 1997, AJ, 113, 1445
Zhang, E., Robinson, E. L., & Nather, R. E. 1986, ApJ, 305, 740